RSC Advances

ROYAL SOCIETY OF CHEMISTRY

www.rsc.org/advances

Graphical abstract:

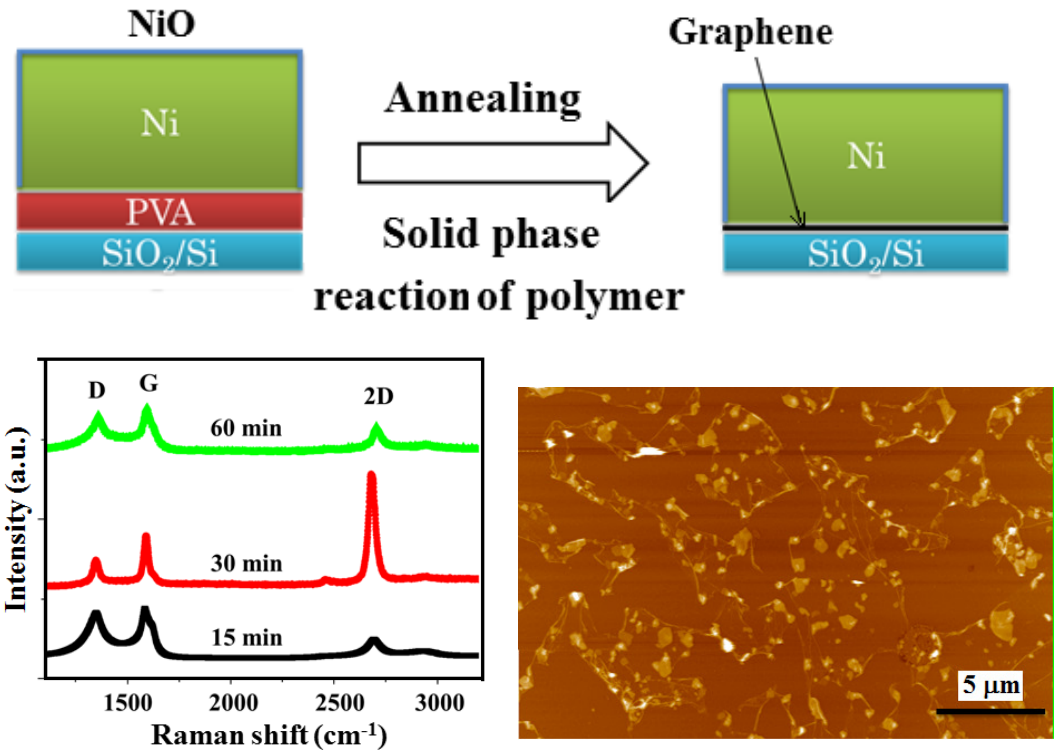

Controllable direct graphene growth process on an insulating substrate (SiO_2/Si and sapphire) by the solid phase reaction of polymer (polyvinyl alcohol) thin film.

Controlling direct growth of graphene on insulating substrate by solid phase reaction of polymer layer

Golap Kalita[*,1,2], Takatoshi Sugiura[2], Yuji Wakamatsu[2], Ryo Hirano[2], Masaki Tanemura[2]

[1]Center for Fostering Young and Innovative Researchers, Nagoya Institute of Technology, Gokiso-cho, Nagoya 466-8555, Japan

[2]Department of Frontier Materials, Nagoya Institute of Technology, Gokiso-cho, Nagoya 466-8555, Japan

*Corresponding author address: Phone/Fax: +81-52-735-5216 E-mail: kalita.golap@nitech.ac.jp (GK)

Abstract

Here, we report controllable direct graphene growth process on an insulating substrate (SiO_2/Si and sapphire) by the solid phase reaction of a polymer layer. Water soluble polyvinyl alcohol (PVA) was spin coated on the SiO_2/Si substrate and graphitized in presence of a Ni catalyst cap layer. Graphene growth occurs with decomposition and dehydrognetaion of the polymer layer with metal catalyzation. The role of gas atmosphere,

temperature, thickness of polymer and catalyst layers are investigated in the solid phase reaction process for graphene nucleation and growth. Formation of graphene flakes directly on the substrate surface is confirmed by Raman spectroscopy, optical and atomic force microscopy analysis. The as-synthesized graphene flakes interconnect each other to create a network like structure. In the growth process, decomposing the polymeric film at an elevated temperature, atomic carbons can diffuse and segregate at the Ni/substrate interface to create the graphene structure. The developed direct growth process of graphene structure using a simple polymer by a solid phase reaction can be significant for device integration.

1. Introduction

Considering the exceptional physical properties of graphene[1-3], synthesis of high quality graphene based materials is of great interest for integration in electronic devices. Graphene has been derived or synthesized by mechanical exfoliation of highly oriented pyrolytic graphite (HOPG)[4], thermal decomposition of silicon carbide[5], reduction of exfoliated graphene oxide[6] and chemical vapor deposition (CVD).[7-9] Among these various approaches, CVD technique is the most versatile to grow high quality large-area graphene on a metal catalytic substrate.[10-12] Synthesis of continuous graphene film, patterned structure and individual crystals has been achieved by CVD technique on transition metal substrates.[10-15] Recently, wafer scale single crystal graphene has been synthesized on Ge (110)/Si(110) substrate by a CVD process.[16] The possibility of transferring CVD synthesized graphene film onto an arbitrary substrate led to considerable development in graphene research toward practical applications. On the other hand, synthesis of a transfer-free graphene directly on an insulating substrate can be more promising, thereby eliminating the drawbacks of transfer process.[17-19]

Recently, synthesis of graphene directly on arbitrary substrate for device integration is emerging and getting significant attention.[20-22] Ismach et al. have demonstrated transfer-free synthesis of few-layers graphene on dielectric substrate by a CVD approach owing

to evaporation of Cu catalyst layer during growth process.[23] Similarly, few-layers graphene has been directly obtained on SiO_2/Si substrate by transition metal assisted crystallization of amorphous carbon thin film at an elevated temperature.[24-27] Graphene synthesized by the metal assisted crystallization process has been integrated with Si substrate for fabrication of a Schottky junction.[22] Few-layer graphene has been also synthesized on insulating substrates from polystyrene (PS) and polymethylmetacrylate (PMMA) based polymer films with a metal capping layer.[28,29] Again, poly(phenylcarbyne) has been used for synthesis of two-dimensional freestanding amorphous carbon nanosheets by a pulsed laser ablation process.[30] The use of a simple solution coated polymer film can be very effective and simple for developing patterned structure and selective-area growth of graphene. In contrast to previous studies, we investigate the morphology and structure of directly grown graphene on insulating substrate by the metal assisted graphitization process of a polymer film.

Solid phase reaction process of a PVA thin film and transition metal capped layer is investigated to obtain transfer-free graphene directly on SiO_2/Si and sapphire substrate. Graphene with better structural quality can be obtained by controlling carbon diffusion and segregation in the solid phase reaction process. In this aspect, we report the role of gas atmosphere, temperature, thickness of polymer and catalyst layers in the graphene

nucleation and growth process.

2. Experimental details

In these studies, we used PVA (molecular weight >1500 g/mol, thermal decomposition temperature of ~228°C) as carbon source purchased from Wako chemical. PVA solution in water was spin coated on the preferred substrate (SiO_2/Si and sapphire) with different thicknesses (4.5 and 9.2 nm). Ni catalyst layers with thickness 150 and 200 nm were deposited on the polymer layer by pulse laser ablation process using a Nd:YAG laser (λ=355 nm, energy density of 30 mJ and f=10 Hz). Subsequently, a thin NiO layer (~3 nm) as carbon diffusion barrier was created on the top of Ni by UV ozone treatment. Annealing of NiO/Ni/PVA stacked layers on SiO_2/Si and sapphire substrate was performed at temperature range of 850~990 ^{0}C. The NiO and Ni layers were removed by chemical etching process in a diluted nitric acid solution (30%) and graphene was directly obtained on substrate surface. Figure 1a shows a schematic diagram of the transfer-free graphene synthesis process using spin coated PVA film by the solid phase reaction. Figure 1b shows temperature profile of the annealing and cooling process used for graphene synthesis.

In each step of experiments, morphological and structural analyses of the synthesized material were performed with Raman spectroscopy, optical and atomic force microscopy

(AFM). Raman studies were performed with NRS 3300 Raman spectrometer with laser excitation energy of 532.08 nm from a green laser. The optical microscopy studies were carried out with VHX-5000 digital microscope. AFM studies were performed with a JSPM-5200 scanning probe microscope. Scanning electron microscope (SEM) study was carried out with Hitachi S-4300 operated at an acceleration voltage 20 kv. Sheet resistance of the graphene structure obtained on SiO_2/Si was studied by four probe technique using RT-70V/RG-7C of Napson Corporation.

3. Results and discussion

In the graphene synthesis process, PVA was considered as the starting polymer due to high water solubility and possibility of coating large-area uniform thin film on various substrates. Figure 2a shows an AFM image of PVA coating on SiO_2/Si substrate. Uniform thin film formation with spin coating of PVA solution is observed without any significant roughness. PVA can be the simplest polymer and easiest to fabricate a thin film without using any hazardous organic solvent. Figure 2a shows Raman spectra of PVA thin film comparing with room temperature deposited amorphous carbon film. We observed a broad peak at around 1500 cm^{-1} for the amorphous carbon film, whereas no peaks were observed for the PVA film. The uniform PVA film was coated with Ni catalytic layer and annealed at various temperature to investigate the solid phase reaction process for

graphene growth. Figure 3a shows a Raman spectra of the PVA film after annealing at 900 ^{0}C in Ar atmosphere in presence of top Ni (~150 nm) catalyst layer. Two clear splitted Raman peaks are observed at 1330 and 1580 cm^{-1}, corresponding to disorder-induced D and graphitic G band, respectively. An additional small 2D second-order Raman peak at 2700 cm^{-1} is also observed, corresponding to poor graphitization of the polymer film. Figure 3b-c shows SEM and AFM images of the graphitized polymer film after etching the top Ni layer. The AFM and Raman studies clearly show poor graphitization without any graphene sheet like structure.

Thickness of the Ni layer and annealing temperature were investigated to enhance the quality of graphene. A Ni thin film (>200 nm) and diffusion barrier of NiO (3 nm) was deposited on PVA coated SiO_2/Si substrate. Figure 4a shows Raman spectra of the directly obtained graphene on SiO_2/Si at three different annealing temperature of 900, 950 and 990 ^{0}C. Graphitic G, defect-induced D and second order 2D Raman peaks are observed at 1330, 1584 and 2696 cm^{-1}, respectively. The 2D Raman peak intensity is found to be higher with increasing the growth temperature upto 990 ^{0}C. Graphitization of the polymer layer enhanced with an increase in annealing temperature and a thicker catalyst layer. Figure 4b shows optical microscope image of the graphene structure corresponding to the Raman spectra at three different annealing temperatures. We

observed formation of interconnected graphene flakes like structure directly on SiO_2/Si substrate. Growth of larger graphene flake (~50 μm) is obtained with an increase in annealing temperature. This shows that the graphene growth with solid phase graphitization process of polymer film is significantly influenced by the thickness of the catalyst layer and growth temperature. Figure 4c shows mapping images of D to G and G to 2D peak ratios, indicating growth of few-layers graphene structures with defects. The mapping images confirm homogenous and uniform growth of graphene structures on most part of the SiO_2/Si substrate.

Figure 5a-c shows AFM images of graphene synthesized at three different growth temperatures on SiO_2/Si substrate. The AFM studies showed network like structure of graphene flakes as also observed in optical microscope studies. We obtained formation of smaller graphitic flakes within the graphene sheets at a lower growth temperature. While, much larger and distinct graphene sheets along with smaller graphitic flakes were obtained increasing the growth temperature to 990 ^{0}C. In the growth process, diffusion and segregation of carbon atoms in presence of the catalyst and diffusion barrier layer is effective to grow high quality graphene structures. The profile of a graphene sheet synthesized at 990 ^{0}C is shown in figure 5d. Thickness of the graphene sheets is obtained as around 1.9 nm, corresponding to 5-6 number of graphene layers. In this synthesized

process, the obtained graphene network structure can be significant for direct device applications. The interconnected network graphene structure can be integrated for fabrication of a hybrid solar cell similar to carbon nanotubes network device.[31]

Graphene growth was further analyzed by changing the gas atmosphere. Solid phase reaction of PVA layer coated with NiO/Ni was performed only in H_2 atmosphere for various growth durations. Graphene growth in H_2 atmosphere is achieved at a lower annealing temperature (850 ^{0}C) than that of in Ar atmosphere. Figure 6a shows Raman spectra of the graphene structures for growth duration of 15, 30 and 60 min. Graphitic G, defect-induced D and second order 2D Raman peaks are observed at 1336, 1582 cm^{-1} and 2698 cm^{-1}, respectively. For the annealing duration of 30 min., we observed significantly intense 2D peak than that of the G peak, corresponding to growth of monolayer graphene. The poor graphene quality at a lower growth duration (15 min.) can be explained from ineffective carbon segregation and graphitization process. While, increasing the growth duration significant amounts of defects were also observed. These results clearly show that growth of graphene at interface of catalyst layer and insulating substrate is significantly affected by the carbon atoms diffusion and segregation process. Figure 6b-c shows optical microscope and AFM image of graphene synthesized on SiO_2/Si substrate by solid phase reaction of the PVA film. Graphene structures obtained by annealing H_2

atmosphere show much higher coverage of interconnected graphene flakes. In the growth process, atomic hydrogen can react with the Ni catalyst and PVA thin film to enable high quality graphene growth at the substrate interface. Previously, it has been explained that atomic H_2 can diffuse to catalyst/substrate interface and reacting with the polymer layer at a higher temperature.[19,29,32,33] The graphene with higher coverage and interconnected structure on the insulating substrate shows a sheet resistance of 48 kΩ/sq.

Graphene growth is also investigated at the interface of Ni catalyst layer and a sapphire substrate instead of SiO_2 substrate. The sapphire substrates are insulating, thermally stable and contains less defect density, hence can be suitable substrate for direct graphene growth. Figure 7a shows an optical microscope image of graphene synthesized on sapphire substrate. Growth of large graphene sheets (20-50 μm) along with smaller graphitic flakes is observed. High amount of surface coverage with graphene sheet is also obtained on sapphire substrate. Figure 7b shows Raman spectra at two different positions as shown in the optical microscope image. At position 1, we observed a defect-induced D peak along with the G and 2D peaks at 1336, 1584 and 2698 cm^{-1}, respectively. While, at position 2, significantly reduced defect induced D peak along with the G and 2D peaks can be observed. This shows that the induced defect considerably relate to the number of layers grown at the substrate interface. This can be related to the precipitation process of

the diffused carbon atoms at interface in presence of the polycrystalline Ni grain and grain boundaries. These studies give a clear idea of the graphene growth process directly on insulating substrate with higher surface coverage by the solid phase reaction of polymer thin and caped catalyst layer.

4. Conclusion

We have demonstrated controllable direct growth of graphene structure on an insulting substrate (SiO_2/Si and sapphire) by the solid phase graphitization process of a polymer layer. Water soluble PVA was spin coated on the SiO_2/Si substrate and graphitized at the interface of a Ni catalyst layer and substrate. High amount of surface coverage was obtained by optimizing the thickness of Ni catalyst (>200 nm) and polymer layer (9.2 nm) for graphene growth in the reaction process. The as-synthesized graphene flakes were interconnected each other to create a network like structure. We also observed a strong influence of Ar and H_2 atmosphere in the graphene growth process. Monolayer graphene growth was only obtained in H_2 atmosphere at a lower temperature (850 ^{0}C) than that of Ar atmosphere, attributing to H_2 diffusion in the catalyst/substrate interface to activate carbon atoms for graphene growth. In the graphene growth process, decomposing the polymeric film at an elevated temperature (850-990 ^{0}C) atomic carbon can diffuse and segregate at the Ni/substrate interface to create the graphene structure. The developed

direct growth process of graphene structure using a simple polymer can be significant for practical device fabrication.

Acknowledgments

The work is supported by the funds for the development of human resources in science and technology, Japan.

References

1. A. K. Geim, K. S. Novoselov, *Nature Mater.* 2007, **6**, 183-191.

2. S. V. Morozov, K. S. Novoselov, M. I. Katsnelson, F. Schedin, D. C. Elias, J. A. Jaszczak and A. K. Geim, *Phys. Rev. Lett.*, 2008, **100**, 016602.

3. R. R. Nair, P. Blake, A. N. Grigorenko, K. S. Novoselov, T. J. Booth, T. Stauber, N. M. R. Peres and A. K. Geim, *Science*, 2008, **320**, 1308.

4. K. S. Novoselov, D. Jiang, F. Schedin, T. J. Booth, V. V. Khotkevich, S. V. Morozov and A. K. Geim, *Proc. Natl. Acad. Sci.* 2005, **102**, 10451-10453.

5. C. Berger, Z. Song, X. Li, X. Wu, N. Brown, C. Naud, D. Mayou, T. Li, J. Hass, A. N. Marchenkov, E. H. Conrad, P. N. First and W. A. de Heer, *Science*, 2006, **312**, 1191-1196.

6. S. Stankovich, D. A. Dikin, G. H. B. Dommett, K. M. Kohlhaas, E. J. Zimney, E. A. Stach, R. D. Piner, S. T. Nguyen and R. S. Ruoff, *Nature*, 2006, **442**, 282-286.

7. P. R. Somani, S. P. Somani, M. Umeno, *Chem. Phys. Letts.*, 2006, **430**, 56-59.

8. Q. Yu, J. Lian, S. Siriponglert, H. Li, Y.P. Chen, S. S. Pei, *Appl. Phys. Lett.*, 2008, **93**, 113103.

9. A. Reina, X. Jia, H. John, D. Nezich, H. Son, V. Bulovic, M. S. Dresselhaus and J. Kong *Nano Lett*., 2009, **9**, 30-35.

10. K. S. Kim, Y. Zhao, H. Jang, S. Y. Lee, J. M. Kim, K. S. Kim, J. H. Ahn, P. Kim, J. Y. Choi and B. H. Hong, *Nature*, 2009, **457**, 706-710.

11. X. S. Li, W. W. Cai, J. H. An, S. Kim, J. Nah, D. X. Yang, R. Piner, A. Velamakanni, I. Jung, E. Tutuc, S. K. Banerjee, L. Colombo, and R. S. Ruoff, *Science*, 2009, **324**, 1312-1314.

12. S. Bae, H. K. Kim, Y. Lee, X. Xu, J. Park, Y. Zheng, J. Balakrishnan, D. Im, T. Lei, Y. Song, Y. Kim, K. Kim, B. Ozyimaz, J. Ahn, B. Hong and S. Iijima, *Nat. Nanotechnol.*, 2010, **5**, 574-578.

13. Z. Sun, Z. Yan, J. Yao, E. Beitler, Y. Zhu and J. M. Tour, *Nature* 2010, **468**, 549–52.

14. X. Li, C. W. Magnuson, A. Venugopal, R. M. Tromp, J. B. Hannon, E. M. Vogel, L. Colombo and R. S. Ruoff, *J. Am. Chem. Soc.*, 2011, **133**, 2816-2819.

15. Z. Yan, J. Lin, Z. Peng, Z. Sun, Y. Zhu, L. Li, C. Xiang, E. L. Samuel, C. Kittrell and J. M. Tour, *ACS Nano*, 2012, **6**, 9110-9117.

16. J. H. Lee, E. K. Lee, W. J. Joo, Y. Jang, B. S. Kim, J. Y. Lim, S. H. Choi, S. J. Ahn, J. R. Ahn, M. H. Park, C. W. Yang, B. L. Choi, S.W. Hwang and D. Whang, *Science*, 2014, **344**, 286-289.

17. G. Kalita, M. Masahiro, H. Uchida, K. Wakita and M. Umeno, *J. Mater. Chem.*, 2010, **20**, 9713-9717.

18. Z. Yan, Z. Peng, Z. Sun, J. Yao, Y. Zhu, Z. Liu, P. M. Ajayan and J. M. Tour, *ACS Nano*, 2011, **5**, 8187-8192.

19. C. Y. Su, A. Y. Lu, C. Y. Wu, Y. T. Li, K. K. Liu, W. Zhang, S. Y. Lin, Z. Y. Juang, Y. L. Zhong, F. R. Chen and L.J. Li, *Nano Lett.*, 2011, **11**, 3612-3616.

20. Y. S. Kim, K. Joo, S. K. Jerng, J. H. Lee, D. Moon, J. Kim, E. Yoon and S. H. Chun, *ACS Nano*, 2014, **8**, 2230-2236.

21. J. Kwak, J. H. Chu, J. K. Choi, S. D. Park, H. Go, S. Y. Kim, K. Park, S. D. Kim, Y. W. Kim, E. Yoon, S. Kodambaka and S. Y. Kwon, *Nature Comm.*, 2012, 3, 645.

22. G. Kalita, R. Hirano, M. E. Ayhan and M. Tanemura, *J. Phys. D: Appl. Phys.*, 2013. **46**, 455103.

23. A. Ismach, C. Druzgalski, S. Penwell, A. Schwartzberg, M. Zheng, A. Javey, J. Bokor and Y. Zhang, *Nano Lett.*, 2010, **10**, 1542–1548.

24. R. Hirano, K. Matsubara, G. Kalita, Y. Hayashia and M. Tanemura, *Nanoscale*, 2012, **4**, 7791-7796.

25. G. Pan, B. Li, M. Heath, D. Horsell, M. L. Wears, L. A. Taan, S. Awan, *Carbon*, 2013, **65**, 349-358.

26. K. Gumi, Y. Ohno, K. Maehashi, K. Inoue and K. Matsumoto, *Jap. Jour. App. Phys.* 2012, **51**, 06FD12.

27. K. Banno, M. Mizuno, K. Fujita, T. Kubo, M. Miyoshi, T. Egawa and T. Soga, *Appl. Phys. Lett.* 2013, **103**, 082112.

28. S. J. Byun, H. Lim, G. Y. Shin, T. H. Han, S. H. Oh, J. H. Ahn, H. C. Choi and T. W. Lee, *J. Phys. Chem. Lett.,* 2011, **2**, 493–497.

29. T. Takami, R. Seino, K. Yamazaki and T. Ogino, *J. Phys. D: Appl. Phys.*, 2014, **47**, 094015.

30. M. Qiana, Y. S. Zhou, Y. Gao, J. B. Park, T. Feng, S. M. Huang, Z. Sun, L. Jiang, Y. F. Lu, *Carbon*, 2011, **49**, 5117–5123.

31. Y. Jia, A. Cao, X. Bai, Z. Li, L. Zhang, N. Guo, J. Wei, K. Wang, H. Zhu, D. Wu and P. M. Ajayan, *Nano Lett.*, 2011, **11**, 1901-1905.

32. Y. Zhang, Z. Li, P. Kim, L. Zhang and C. Zhou, *ACS Nano*, 2012, **6**, 126-132.

33. D. Geng, B. Wu, Y. Guo, B. Luo, Y. Xue, J. Chen, G. Yu and Y. Liu, *J. Am. Chem. Soc.*, 2013, **135**, 6431-6434.

Figure captions:

Figure 1 (a) Schematic diagram of the transfer-free graphene synthesis process using spin coated PVA layer by the solid phase reaction process. (b) Annealing temperature profile and cooling rate for graphene synthesis.

Figure 2 (a) AFM image of the spin coated PVA film on SiO_2/Si substrate. (b) Raman spectra of a PVA thin film comparing with room temperature deposited amorphous carbon film.

Figure 3 (a) Raman spectra of a PVA film after annealing at 900 ^{0}C in Ar atmosphere in presence of top Ni (~100 nm) catalyst layer. (b) SEM and (c) AFM images of the graphitized polymer film after etching the top Ni layer.

Figure 4 (a) Raman spectra of the directly grown graphene on SiO_2/Si at three different annealing temperature of 900, 950 and 990 ^{0}C. (b) Optical microscope image of graphene structure corresponding to the Raman spectra. (c) Mapping image of D to G and G to 2D peak ratio, indicating growth of few layer graphene structures with presence of defects.

Figure 5 AFM images of the graphene synthesized at (a) 850, (b) 900 and (c) 990 ^{0}C temperature on SiO_2/Si substrate. The AFM studies show network like structure of the graphene flakes as also observed by the optical microscope studies.

Figure 6 (a) Raman spectra of graphene synthesized for 15, 30 and 60 min. at 850 ^{0}C

growth temperature. (b) Optical microscope and (c) AFM image of the graphene synthesized on SiO_2/Si substrate at 850 ^{0}C for a growth duration of 30 min.

Figure 7 (a) Optical microscope image of graphene synthesized on sapphire substrate. Growth of large graphene sheets (20-50 μm) along with smaller graphitic flakes are observed. (b) Raman spectra of the synthesized graphene sheet at position 1 and 2 of optical microscope image.

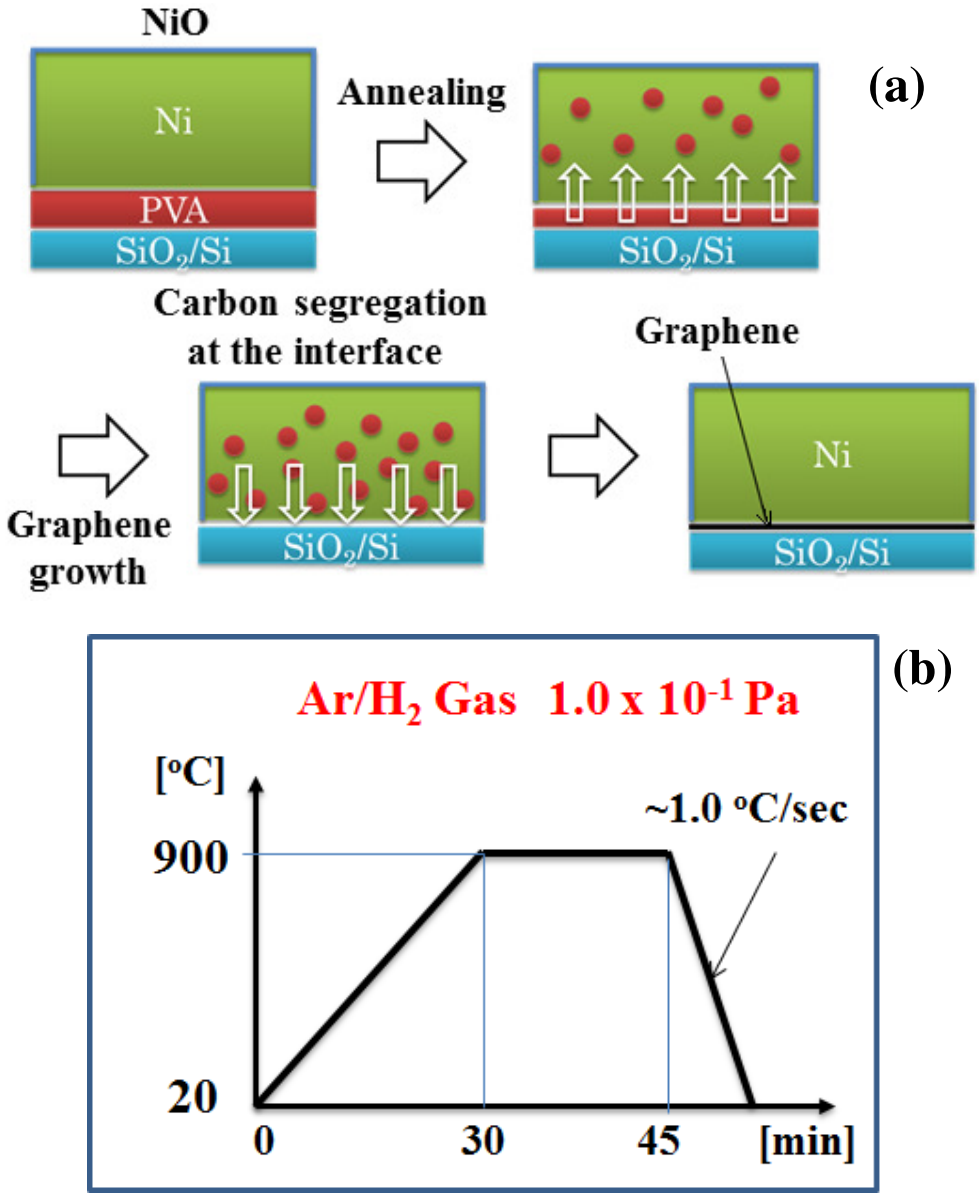

Figure 1

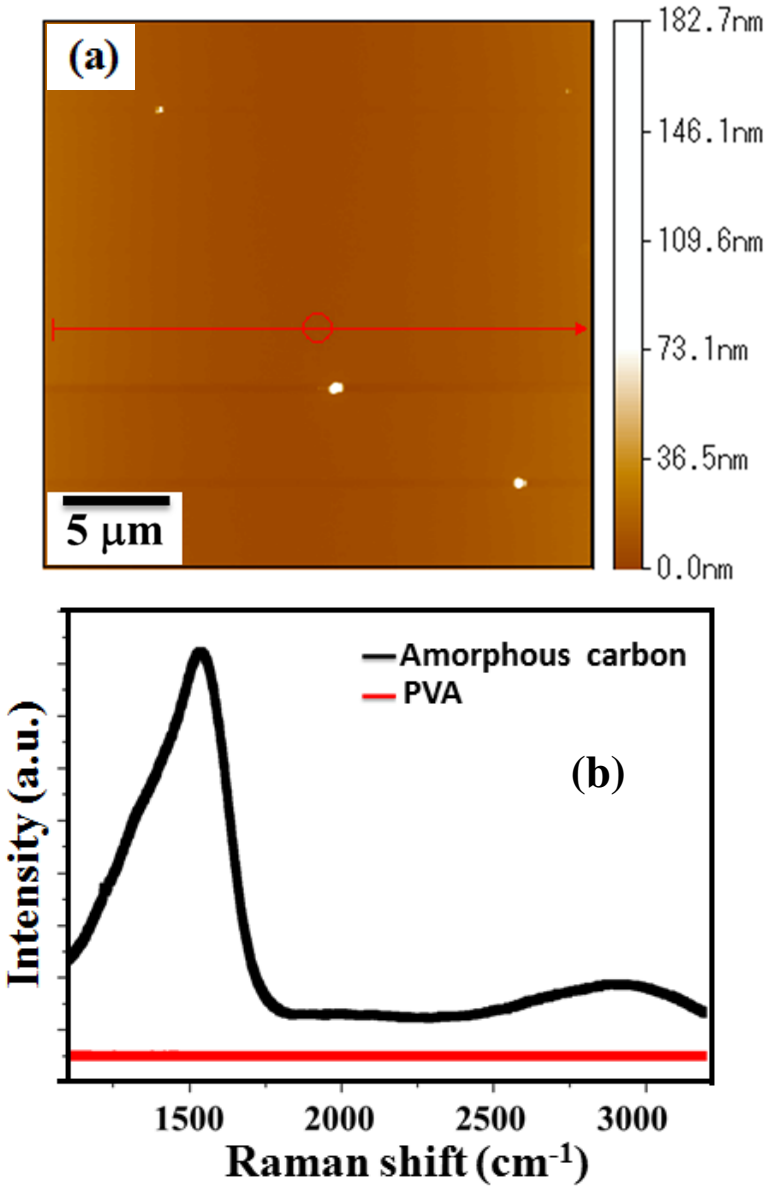

Figure 2

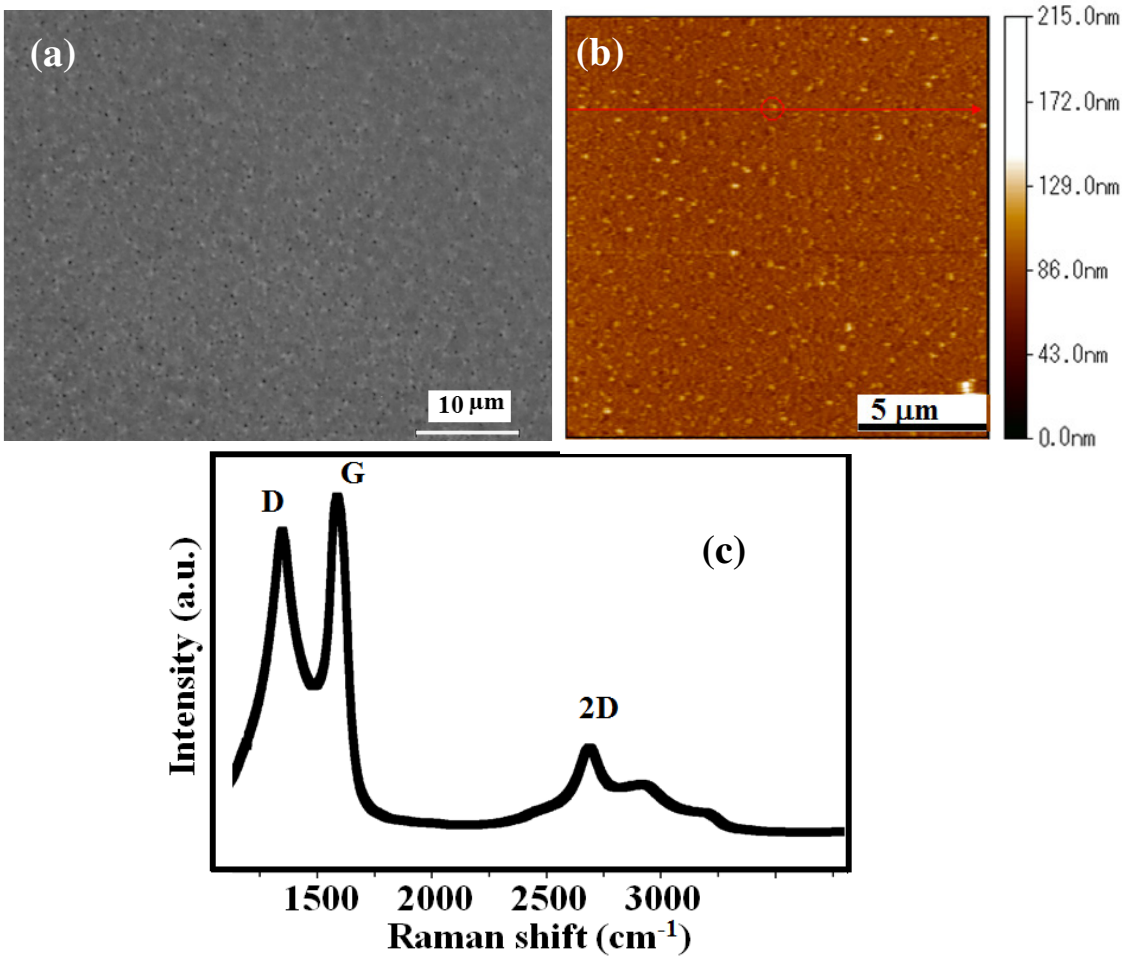

Figure 3

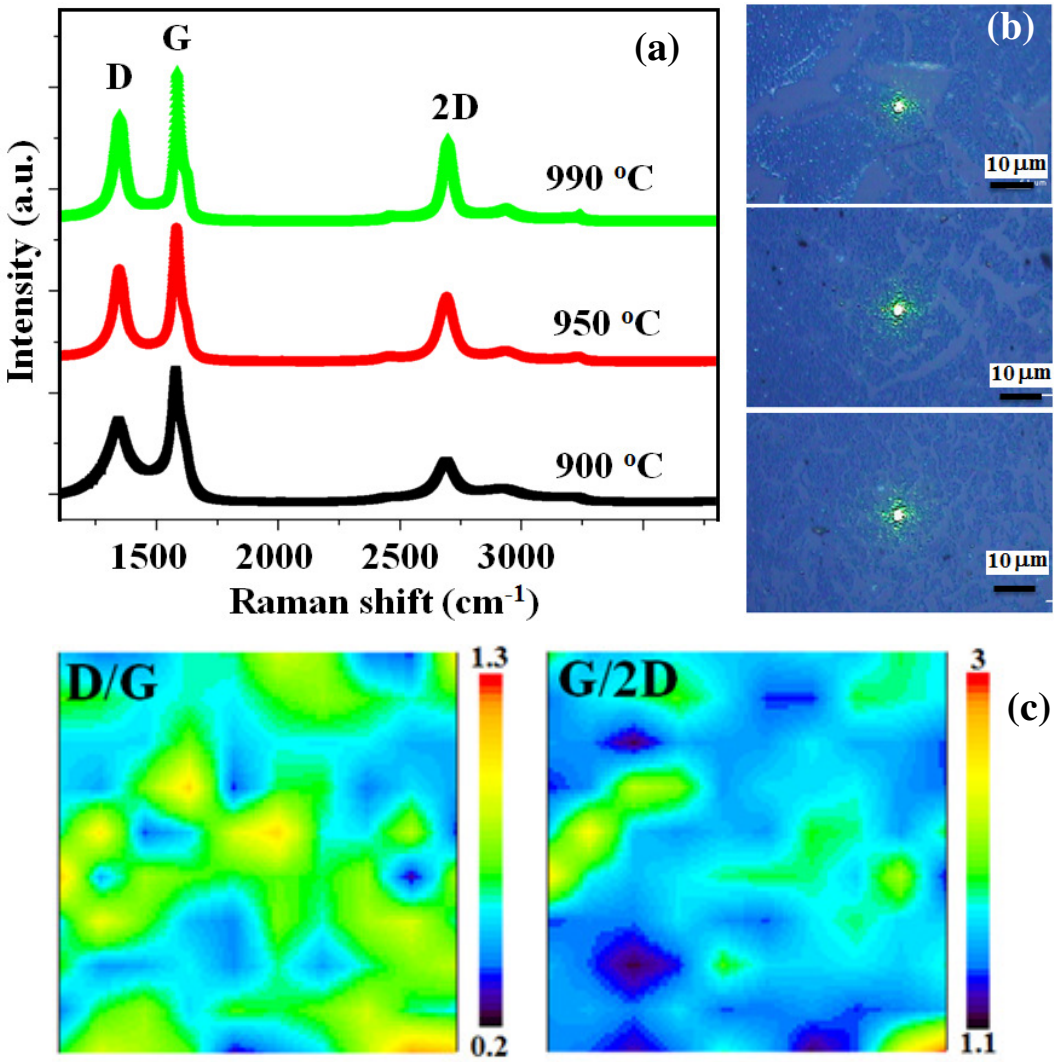

Figure 4

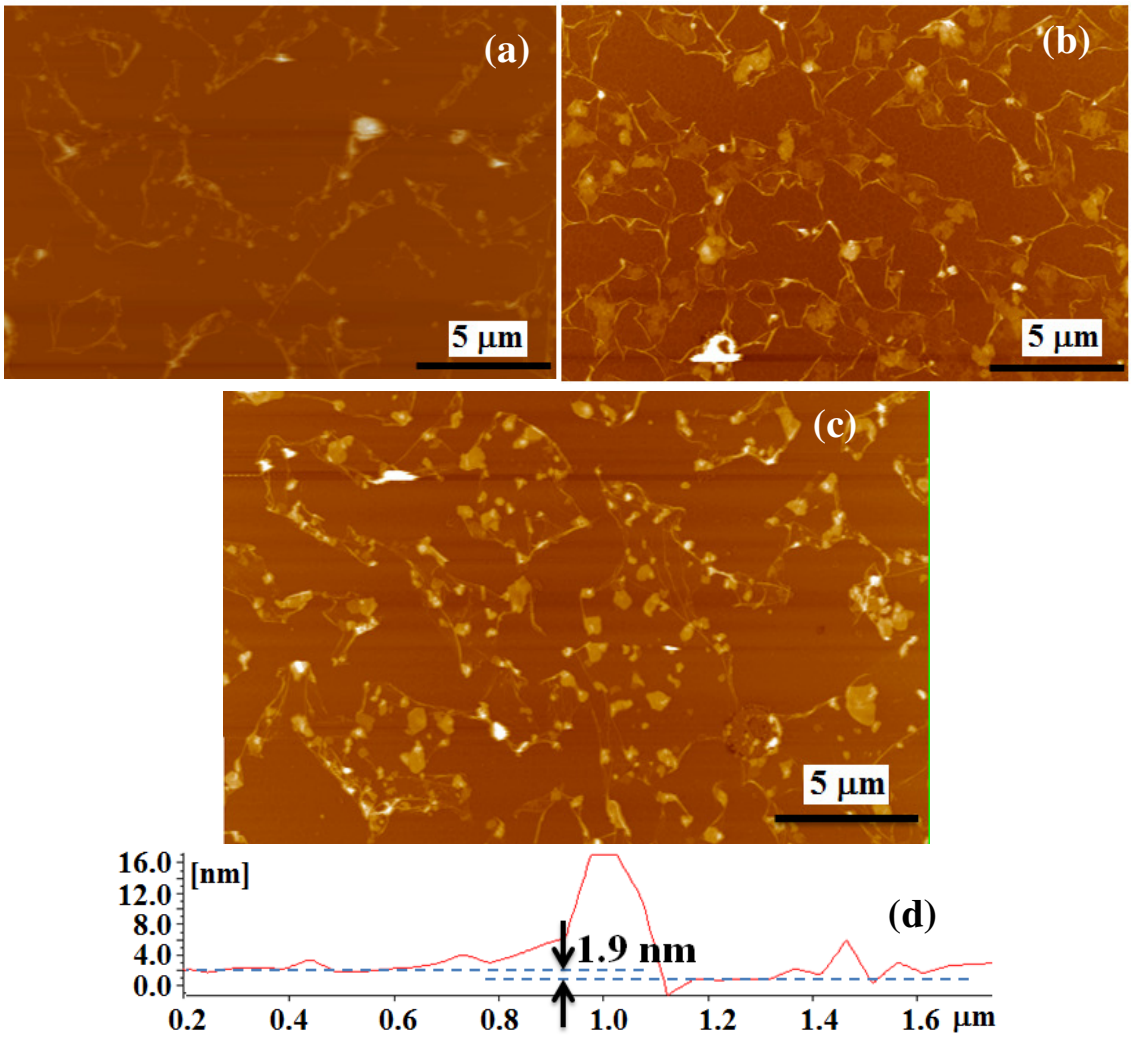

Figure 5

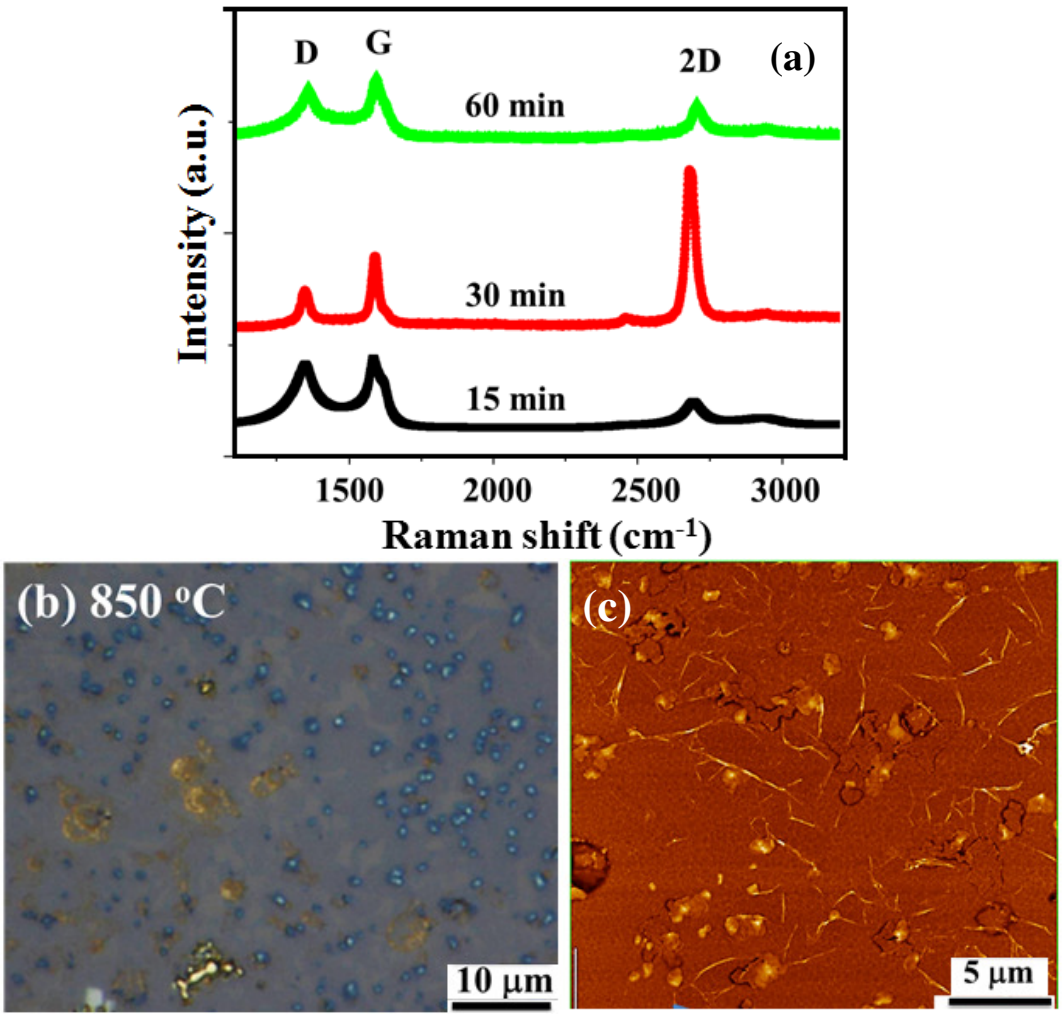

Figure 6

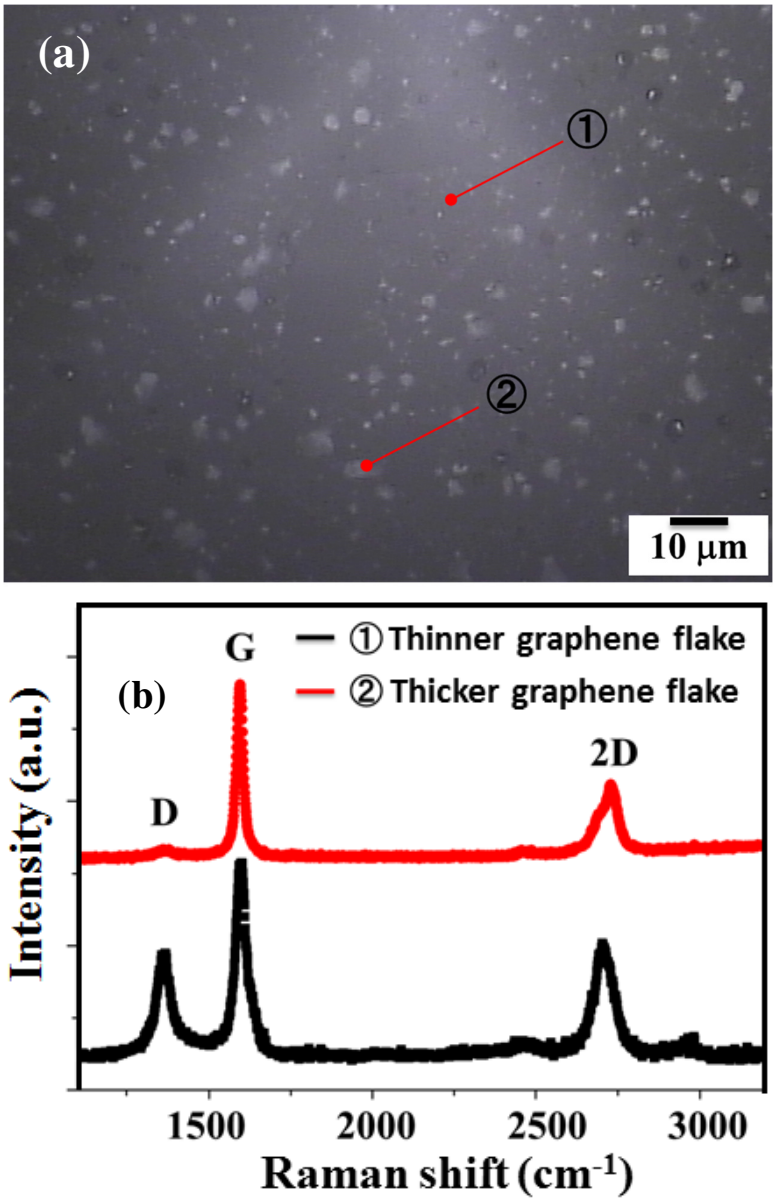

Figure 7